

New $MgO-H_2O$ compounds at extreme conditions

Lanci Guo(郭兰慈) and Jurong Zhang(张车荣)

Citation: Chin. Phys. B, 2023, 32 (**7**): 076201. DOI: 10.1088/1674-1056/ace035
Journal homepage: http://cpb.iphy.ac.cn; http://iopscience.iop.org/cpb

What follows is a list of articles you may be interested in

Pressure-induced structural transition and low-temperature recovery of sodium pentazolate

Zitong Zhao(赵梓彤), Ran Liu(刘然), Linlin Guo(郭琳琳), Shuang Liu(刘爽), Minghong Sui(隋明宏), Bo Liu(刘波), Zhen Yao(姚震), Peng Wang(王鹏), and Bingbing Liu(刘冰冰)
Chin. Phys. B, 2023, 32 (**4**): 046202. DOI: 10.1088/1674-1056/acb917

In situ study of calcite-III dimorphism using dynamic diamond anvil cell

Xia Zhao(赵霞), Sheng-Hua Mei(梅升华), Zhi Zheng(郑直), Yue Gao(高悦), Jiang-Zhi Chen(陈姜智), Yue-Gao Liu(刘月高), Jian-Guo Sun(孙建国), Yan Li(李艳), and Jian-Hui Sun(孙建辉)
Chin. Phys. B, 2022, 31 (**9**): 096201. DOI: 10.1088/1674-1056/ac6157

High-pressure study of topological semimetals XCd_2Sb_2 (X = Eu and Yb)

Chuchu Zhu(朱楚楚), Hao Su(苏豪), Erjian Cheng(程二建), Lin Guo(郭琳), Binglin Pan(泮炳霖), Yeyu Huang(黄烨煜), Jiamin Ni(倪佳敏), Yanfeng Guo(郭艳峰), Xiaofan Yang(杨小帆), and Shiyan Li(李世燕)
Chin. Phys. B, 2022, 31 (**7**): 076201. DOI: 10.1088/1674-1056/ac7212

Bandgap evolution of Mg_3N_2 under pressure: Experimental and theoretical studies

Gang Wu(吴刚), Lu Wang(王璐), Kuo Bao(包括), Xianli Li(李贤丽), Sheng Wang(王升), and Chunhong Xu(徐春红)
Chin. Phys. B, 2022, 31 (**6**): 066205. DOI: 10.1088/1674-1056/ac4cbe

Pressure-induced phase transitions in the ZrXY (X= Si, Ge, Sn;Y= S, Se, Te) family compounds

Qun Chen(陈群), Juefei Wu(吴珏霏), Tong Chen(陈统), Xiaomeng Wang(王晓梦), Chi Ding(丁弛), Tianheng Huang(黄天衡), Qing Lu(鲁清), and Jian Sun(孙建)
Chin. Phys. B, 2022, 31 (**5**): 056201. DOI: 10.1088/1674-1056/ac5989

New $MgO–H_2O$ compounds at extreme conditions

Lanci Guo(郭兰慈) and Jurong Zhang(张车荣)†

School of Physics and Electronics, Shandong Normal University, Jinan 250014, *China*

(Received 17 April 2023; revised manuscript received 20 June 2023; accepted manuscript online 21 June 2023)

The reaction of water and other materials has been the central topic under high-pressure physics research, because the Earth, super-Earth, Uranus, Neptune and other planets contain a great amount of water inside. However, the reaction between star-rich MgO and water under ultra-high pressure remains still poorly understood. Here, using *ab initio* evolutionary structure prediction researches of the structures of $MgO–H_2O$ system at 300 GPa–600 GPa, we find that $(MgO)_2H_2O$ and $MgO(H_2O)_2$ could become stable. The $(MgO)_2H_2O$ compounds may be an important component of super-Earth and the ice-rock boundary of Uranus and Neptune. Furthermore, it may be the reservoir under high pressure before the forming of the Earth's core or other super-Earths. The current findings could expand our knowledge and improve our understanding of the evolution and composition of planets.

Keywords: high pressure, structure prediction, crystal structure

PACS: 62.50.–p, 71.20.–b, 88.10.gc, 64.70.K **DOI:** 10.1088/1674-1056/ace035

1. Introduction

Water is abundant in the Earth, Uranus and Neptune and is a vital resource for all life, however, it is not clear how water is inside these planets. Water is mostly stored in the mantle on the Earth,[1,2] however, on Uranus and Neptune, water has separate ice sheets.[3] The study of the source and evolution of water in the body deepens the understanding of the evolution and structure of stars.

It has recently been reported that in the early Earth, when the pressure and mass were high, water may exist in the form of Mg–O–Si–H compounds.[4] As the Earth evolved, the pressure and mass decreased, and the compounds dissolved, then the water was released and poured into the mantle and crust. The sources of water in the interior of giant planet are the same as the Earth, but at higher pressure. This motivate us to explore the stability of aqueous substances at higher pressures. The inner ice mantle layer of Uranus and Neptune stores a large amount of water, and their body cores are stony cores containing a large amount of SiO_2, MgO, $MgSiO_3$ and other minerals.[5,6] However, the interaction between the mantle and its rocky core is rarely studied for its high pressure. Currently, it is known that SiO_2 can react with H_2O to form Si–O–H ternary compounds.[7] The recent report found that the MgO dissolves in H_2O at about 40 GPa, which is in the H_2O-rich mantle layer of Uranus.[8] The reaction of magnesium-containing minerals and water in Uranus and Neptune at the present-day H_2O-rock boundary and under high pressure has not been reported.

The lower mantle makes up 50% of the Earth's volume and contains (Mg, Fe, Al)(Si, Al)O_3 perovskite [or post-perovskite (ppv) and an (Mg, Fe)O ferropericlase].[9–11] MgO is one important compound in planetary mantles, and it reacts with other substances at high pressure is essential for understanding the evolution of the Earth and planetary. The core of Uranus and Neptune is a rock core, which composes a mixture of silicates and iron.[12] MgO compounds have a very large stability interval, MgO is believed to be the NaCl-type,[13] and then transforms into CsCl-type (B2) at 480 GPa until 3 TPa.[14,15] H_2O is the *Pbcm* phase from 300 GPa–600 GPa,[16] H_3O is *Cmca* phase above 450 GPa[17] and H_2O_2 is *Pbca* phase at 450 GPa–600 GPa. The brucite of $Mg(OH)_2$ is a trigonal structure with *P*-3*ma* phase, at 30 GPa and 800 K transforms to *P*-3 phase, and then to $P4_12_12$ phase at 17 GPa.[18] $Mg(OH)_2$ decomposes to MgO and H_2O above about 30 GPa.

In this work, we researched the $MgO–H_2O$ system at high pressure. The $(MgO)_2H_2O$, $Mg(OH)_2$, and $MgO(H_2O)_2$ stoichiometries were completed at high pressure. These results provided theoretical support for understanding Earth's chemical reactions of the water inside the planets.

2. Method

The CALYPSO prediction method and code[19,20] are used in this work, which has been effectively employed in searching crystal structures at high pressure.[21–26] The total-energy and electronic structure are calculated by the density functional theory (DFT) and VASP code.[27] All-electron projector-augmented wave (PAW) method and 800 eV cutoff energy are used in the Mg–O–H system. $3s^22p^62s^2$, $2s^22p^6$, and 1s are treated as valence electrons for Mg, O, and H elements, respectively. The Perdew–Burke–Ernzerhof (PBE) exchange–correlation functional and the generalized gradient approximation are used.[28,29] Phonon calculations are carried out as implemented in the PHONOPY code.[30]

To determine the phase boundaries between the solid phases, we have performed calculations to determine the

†Corresponding author. E-mail: zjr@calypso.cn

© 2023 Chinese Physical Society and IOP Publishing Ltd

Gibbs free energy $G(T,P) = \min_V[U(V)+PV+F_{\text{phonon}}(T,V)]$, where U, P, V, and F_{phonon} are energy, pressure, volume and phonon free energy, respectively. The vibrational energy and entropy are obtained from lattice dynamic calculations using harmonic approximation as implemented in the PHONOPY code. $F_{\text{phonon}}(T,V) = k_{\text{B}}T\int_0^{\infty} g(\omega,V)\ln[2\sinh(\frac{\hbar\omega}{2k_{\text{B}}T})]\,\text{d}\omega$, where $g(\omega,V)$ is the phonon density of states at frequency ω and volume V. The minimal value of G is found at the equilibrium volume for a given T and P.

3. Results

For a better understanding new Mg–O–H system, we have predicted the 1 f.u.–4 f.u. structures of $(MgO)_2H_2O$, MgO–H_2O, and $MgO(H_2O)_2$ at 300 GPa, 400 GPa, and 600 GPa. MgO–H_2O and $MgO(H_2O)_2$ of the Mg–O–H system are found at 100 GPa–600 GPa. The ternary phase diagrams of Mg–H–O at 400 GPa and 600 GPa are shown in Figs. 1(a) and 1(b). We predict three different ratios $MgO(H_2O)_2$, $(MgO)_2H_2O$, and $Mg(OH)_2$. The structure of $MgO(H_2O)_3$ compound is from the previous report.[31] There are only $MgO(H_2O)_3$, $MgO(H_2O)_2$, and $(MgO)_2H_2O$ stable with the black balls in the ternary phase diagram and $Mg(OH)_2$ is unstable with the red ball. The convex hull of the three different compounds relative to H_2O and MgO is shown in Fig. 1(c) at 300 GPa, 400 GPa, and 600 GPa. $MgO(H_2O)_3$ is a stable compound at 300 GPa. $MgO(H_2O)_3$, $MgO(H_2O)_2$, and $(MgO)_2H_2O$ are in solid line with the convex-hull meaning that they do not decompose at high pressure with respect to possible binary and elemental elements and they are thermodynamically stable at 600 GPa. It should be noted that the $Mg(OH)_2$ compound is stable relative to MgO and H_2O, however, it breaks down according to the others stable compounds at 400 GPa and 600 GPa. This contradicts the previously reported knowledge that $Mg(OH)_2$ compounds decompose into MgO and H_2O at 33 GPa.

The stable ranges of the two stable phases are shown in Fig. 1(d), *Pnma* phase of $(MgO)_2H_2O$ is stable above 365 GPa and $C222_1$ of $MgO(H_2O)_2$ is stable above 598 GPa. We calculate the phonon dispersions of $(MgO)_2H_2O$ and $MgO(H_2O)_2$ at 400 GPa and 600 GPa as shown in Fig. S1. There are no imaginary frequencies in the whole Brillouin zone of $(MgO)_2H_2O$ and $MgO(H_2O)_2$ and clarify the dynamically stable properties.

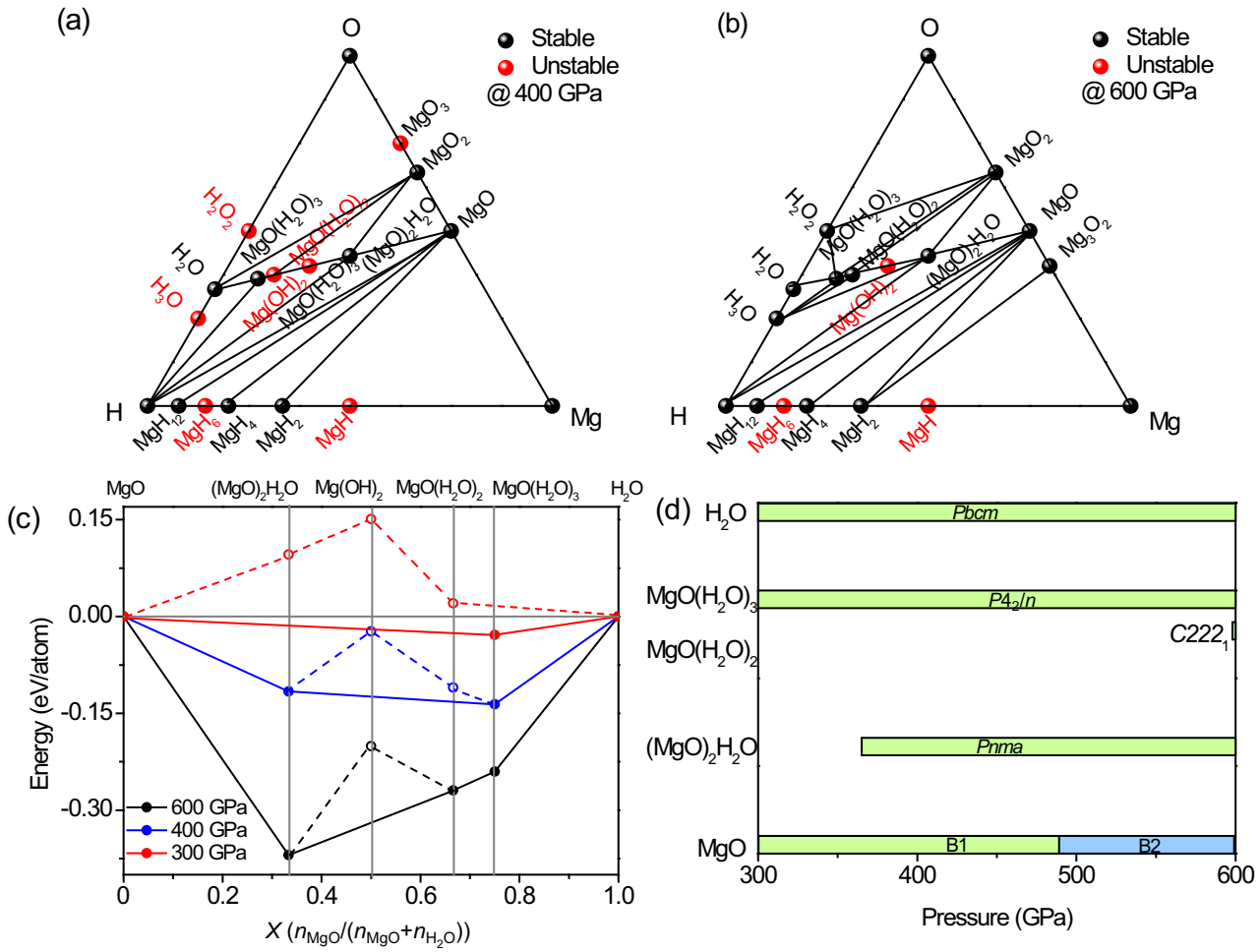


Fig. 1. The stable properties and crystal structures of $(MgO)_2H_2O$, MgO–H_2O, $MgO(H_2O)_2$, and $MgO(H_2O)_3$ compound systems. (a) $(MgO)_2H_2O$, $MgO(H_2O)_2$, and $MgO(H_2O)_3$ compound phase diagrams at 400 GPa. (b) $(MgO)_2H_2O$ and $MgO(H_2O)_2$ compound phase diagrams at 600 GPa. Black circles are the stable and red are unstable structures. (c) The convex hull of MgO–H_2O system. (d) The stable ranges for $(MgO)_2H_2O$ and $MgO(H_2O)_2$ systems.

The crystal structures of $(MgO)_2H_2O$ and $MgO(H_2O)_2$ are shown in Figs. 2(a) and 2(b). The structural, stability, bonding, and electronic properties are analyzed at 400 GPa. The $(MgO)_2H_2O$ phase crystallizes an orthogonal structure (space group *Pnma*, 4 f.u./cell) and exhibits an MgO_8H_8 frame with one Mg atom linked to eight O atoms and O atoms linked to 1–2 H atoms (OH or OH_2 frames) forming Mg–O bonds and O–H bonds. There are two types of hydrogen atoms, two types of magnesium atoms, and one type of oxygen atom in this structure. The $MgO(H_2O)_2$ builds an orthogonal structure (space group $C222_1$, 4 f.u. per cell) containing MgO_9 units with one O atom linked to two H atoms (OH_2 frame) or one O atom linked to four H atoms (OH_4 frame). There is one type of hydrogen atom in this structure, one type of magnesium atom, and two types of oxygen atoms. The Mg–O bonds length of $MgO(H_2O)_2$ and $(MgO)_2H_2O$ are all 1.74 Å–1.88 Å. The covalent O–H bonds length of $(MgO)_2H_2O$ and $MgO(H_2O)_2$ are 1.04 Å–1.15 Å and 0.98 Å–1.19 Å, respectively, compared with ∼ 1.01 Å for $P4_12_12$ of $Mg(OH)_2$.[18] For $MgO(H_2O)_2$ phase the coordination number of Mg is nine, which is rarely seen in minerals, the only previous report was in the compound β-$Mg_2SiO_5H_2$. The coordination of Mg in $MgO(H_2O)_2$is the same as well as proved in the β-$Mg_2SiO_5H_2$[4] compound. The density of $(MgO)_2H_2O$ and $MgO(H_2O)_2$ is 6.47 g/cm^3 and 5.64 g/cm^3, respectively. Furthermore, $(MgO)_2H_2O$ and $(MgO)_2H_2O$ contain 18.36 wt.% and 23.68 wt.% of water, which is larger than $Mg_2SiO_5H_2$ of 11.4 wt.%.

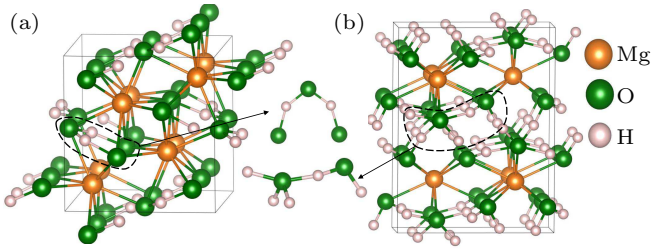


Fig. 2. The crystal structure of (a) the *Pnma* phase of $(MgO)_2H_2O$ compound; (b) the $C222_1$ of $MgO(H_2O)_2$ compound. Detailed structural information is provided in Table S1 of supporting materials.

4. Properties

The projected density of states (PDOS) and band are calculated at 400 GPa as shown in Fig. 3. The PDOS and band of predicted structures reveal the properties of the insulator feature of $MgO(H_2O)_2$ and $(MgO)_2H_2O$ compounds. The bandgaps of $MgO(H_2O)_2$ and $(MgO)_2H_2O$ are 8.21 eV and 7.93 eV at 400 GPa, respectively. In order to analyze the bonding nature of the stable compounds, the electron localization function (ELF) calculation also be analyzed as shown in Fig. 4. In the new compounds, there are OH, OH_2 and OH_4 three different OH frames. The O–H bond of OH_2 frames is a conventional covalent bond for charge localization between the nearest H and O atoms. The O–H bond in OH and OH_4 frames is a weak covalent bond with a longer bonding length (1.128 Å–1.187 Å) than that in the OH_2 frames as shown in Fig. 4. However, there is less localized changes among the Mg–O bonds, suggesting an ionicity between Mg and O atoms. There is a charge transfer of Mg atom 1.32*e* and H 0.62*e* to O at 400 GPa, indicating the ionic property between Mg and O atoms.

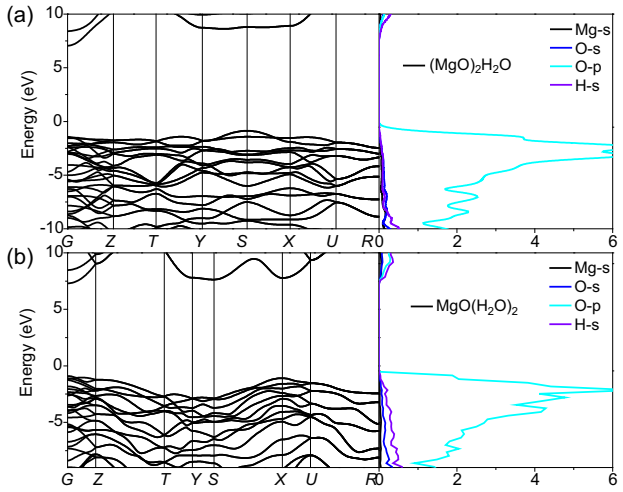


Fig. 3. The calculated PDOS and band of $(MgO)_2H_2O$ and $MgO(H_2O)_2$ compounds at high pressures.

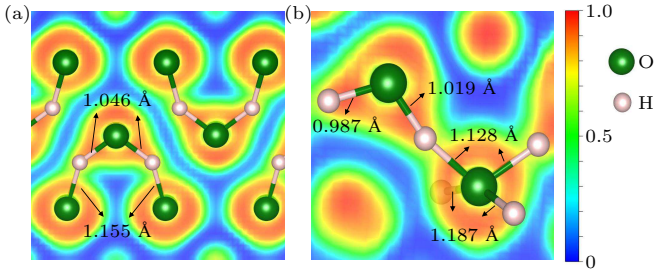


Fig. 4. Calculated ELF at 400 GPa for (a) the *Pnma*-$(MgO)_2H_2O$ phase on (2 1 0) plane and (b) $C222_1$-$MgO(H_2O)_2$ phase on (−5 −1 0.1) plane.

The *H*–*P* (high pressure and high temperature) phase is shown in Figs. 5(a) and 5(b) with respect to $2MgO + H_2O$ of $(MgO)_2H_2O$ and $MgO + 2H_2O$ of $MgO(H_2O)_2$. $MgO(H_2O)_2$ is stable from ∼ 345 GPa–600 GPa and ∼ 0 K–6000 K and $(MgO)_2H_2O$ is stable ∼ 314 GPa–600 GPa and ∼ 0 K–6000 K, which under conditions of Uranus, Neptune, the proto-Earth and super-Earth. Furthermore, we find that $(MgO)_2H_2O$ and $MgO(H_2O)_2$ compounds exhibit the superionic, solid and liquid states of matter as shown in Fig. 5. The superionic state is that H diffuses freely, O and Mg atoms are on the equilibrium sites. A solid state is when all atoms are on their equilibrium sites. Liquid state is that all atoms diffuse freely. The mean squared displacements (MSD) of hydrogen, oxygen, and magnesium atoms for the different states of $(MgO)_2H_2O$ phase are shown in Fig. S2. The MSD of the diffuse freely element is a line that slopes over time, while the vibrate on the equilibrium position element is a line that balances over time. The phase boundaries of different states of $(MgO)_2H_2O$ and $MgO(H_2O)_2$ are identified by MSD (Fig. 5). The isentropes of Neptune and Uranus proposed[32] are also shown in Fig. 5. The temperature

of solid states turns to superionic about 1000 K, and transforms from the superionic state to a liquid state in the temperature range ∼ 5000 K–6000 K with pressure from 300 GPa to 600 GPa of $MgO(H_2O)_2$. Mg and O elements of $(MgO)_2H_2O$ deviate from their equilibrium positions over a nearly identical range of temperatures and pressures. The Mg–O framework is important for the stability of $(MgO)_2H_2O$. The internal temperature and pressure curves of Uranus and Neptune are also shown in Fig. 5 and partially coincide with the liquid and superionic states of $(MgO)_2H_2O$ and $MgO(H_2O)_2$, respectively. The *P*–*T* conditions spanning of reference model for ice layer of Uranus and Neptune are ∼ 20 GPa–600 GPa and ∼ 2000 K–7000 K. Through the above analysis, the superionic regions of $(MgO)_2H_2O$ and liquid region $MgO(H_2O)_2$ may be in the deep mantle or mentle-core boundary of Uranus and Neptune's interior, so they may be components of these giants. This also indirectly proves that the core-mantle boundary of Uranus and Neptune is blurry because water can react with MgO in the Earth's core, as previously reported.

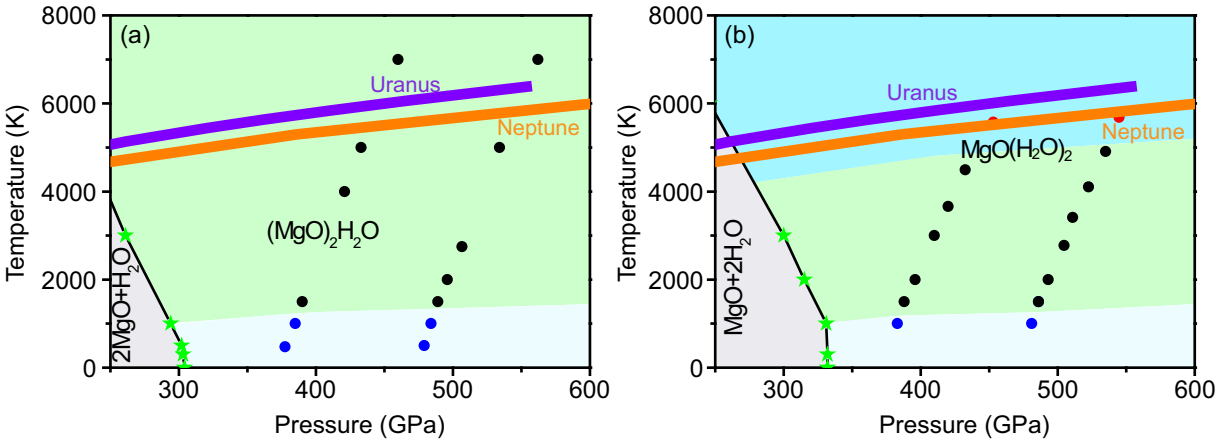


Fig. 5. The pressure–temperature stability field of $(MgO)_2H_2O$ and $MgO(H_2O)_2$ relative to MgO and H_2O. The solid black line is the decomposition curve. Solid, superionic states and liquid phases are marked by blue, black, and red circles. The boundary made up of black lines and fluorescent stars are the decomposition line of the compound with respect to MgO and H_2O. Purple line and origin line are Uranus and Neptune, respectively.

The diffusion coefficient of H of $(MgO)_2H_2O$ superionic state is $D_H = 2.8 \times 10^{-8}$ m^2/s at 446 GPa, 6000 K. We calculate the electrical conductivity by Nernst–Einstein equation $\sigma = q_H^2 N_H D_H / V k_B T$, where q_H, V, N_H are the charge of the hydrogen ion, the volume of the cell, the number of H atoms in the cell, respectively. The electrical conductivity of superionic phases $(MgO)_2H_2O$ phase at a density of 6.47 g/cm^3 and at 446 GPa and 6000 K is around 6.84 S/cm, which is similar to Si–O–H compound in the same temperature and pressure but the order of magnitude smaller than that of number superionic water.[33] Therefore the $(MgO)_2H_2O$ compound affects magnetic field and could also be similar to the Si–O–H compound in the same *P*–*T* range but should be weaker than that from the superionic ice in the same condition. Previous research has shown that the nondipolar and the nonaxisymmetric magnetic fields of Uranus and Neptune have been suggested to come from metallic mixtures,[34] metallic fluid hydrogen,[35] superionic ice,[6] fluid trihydrogen oxide[17] and recently silica-water compound[7] proposed. The $(MgO)_2H_2O$ superionic states may be one possibility for explaining the anomalous magnetic fields of Uranus and Neptune as well as silica-water.

Before the core-mantle separation, Mg slinks into the Earth and pressures above 300 GPa, $(MgO)_2H_2O$ and $MgO(H_2O)_2$ likely at those pressure as well the $Mg_2SiO_5H_2$. It may play the same role as $Mg_2SiO_5H_2$ in storing water in the early Earth.[4] The water may store in $(MgO)_2H_2O$ before the core formation. As the core grows, $(MgO)_2H_2O$ is no longer stable at lower pressure and has to dissociate $(MgO)_2H_2O \rightarrow 2MgO + H_2O$.

Previous research reports there are many super-Earths with mass 1–10 times larger than our Earth outside the solar system.[36] For these super-Earths, the core-boundary pressure is also larger than the Earth, such as a super-Earth with 3 Earth masses is predicted to have a core-boundary pressure of 500 GPa.[37] For these exoplanets, $(MgO)_2H_2O$ with *P*–*T* stable range should exist as a water reservoir in the early Earth.

5. Conclusion

We have identified $(MgO)_2H_2O$ and $MgO(H_2O)$ are thermodynamically stable above 300 GPa and over wide ranges of temperatures and are thus viable inside early Earth during its initial stages of differentiation. This discovery offers insights into the interconnecting substance between the mantle and its rocky core of Uranus and Neptune. The $(MgO)_2H_2O$ may be a water reservoir for the proto-Earth or the super-Earths. The present results also have broad implications for the interpretation and elucidation of physical and chemical processes of the proto-Earth, Uranus, Neptune and super-Earth.

When we submitted our manuscript, we are aware of another similar work which is published in *Nature Communications*.[31]

Acknowledgments

Project supported by the National Natural Science Foundation of China (Grant Nos. 12204280 and 12147135), the Natural Science Foundation of Shandong Province of China (Grant No. ZR202103010004), and the Postdoctoral Science Foundation of China (Grant No. 2021M691980).

References

[1] Pearson D, Brenker F, Nestola F, McNeill J, Nasdala L, Hutchison M, Matveev S, Mather K, Silversmit G and Schmitz S 2014 *Nature* **507** 221
[2] Ohtani E 2020 *Natl. Sci. Rev.* **7** 224
[3] Hubbard W 1981 *Science* **214** 145
[4] Li H F, Oganov A R, Cui H, Zhou X F, Dong X and Wang H T 2022 *Phys. Rev. Lett.* **128** 035703
[5] Guillot T 2005 *Annu. Rev. Earth Planet. Sci.* **33** 493
[6] Redmer R, Mattsson T R, Nettelmann N and French M 2011 *Icar* **211** 798
[7] Gao H, Liu C, Shi J, Pan S, Huang T, Lu X, Wang H T, Xing D and Sun J 2022 *Phys. Rev. Lett.* **128** 035702
[8] Kim T, Chariton S, Prakapenka V, Pakhomova A, Liermann H P, Liu Z, Speziale S, Shim S H and Lee Y 2021 *Nat. Astron.* **5** 815
[9] Fiquet G 2001 *Z. Krist-Cryst. Mater.* **216** 248
[10] Immoor J, Miyagi L, Liermann H P, Speziale S, Schulze K, Buchen J, Kurnosov A and Marquardt H 2022 *Nature* **603** 276
[11] McDonough W F and Sun S S 1995 *Chem. Geol.* **120** 223
[12] Podolak M, Weizman A and Marley M 1995 *Planet. Space Sci.* **43** 1517
[13] Duffy T S, Hemley R J and Mao H k 1995 *Phys. Rev. Lett.* **74** 1371
[14] Zhu Q, Oganov A R and Lyakhov A O 2013 *Phys. Chem. Chem. Phys.* **15** 7696
[15] Belonoshko A B, Arapan S, Martonak R and Rosengren A 2010 *Phys. Rev. B* **81** 054110
[16] Benoit M, Bernasconi M, Focher P and Parrinello M 1996 *Phys. Rev. Lett.* **76** 2934
[17] Huang P, Liu H, Lv J, Li Q, Long C, Wang Y, Chen C, Hemley R J and Ma Y 2020 *Proc. Natl. Acad. Sci. USA* **117** 5638
[18] Hermann A and Mookherjee M 2016 *Proc. Natl. Acad. Sci. USA* **113** 13971
[19] Wang Y C, Lv J, Zhu L and Ma Y M 2010 *Phys. Rev. B* **82** 094116
[20] Wang Y, Lv J, Zhu L and Ma Y 2012 *Comput. Phys. Commun.* **183** 2063
[21] Zhang J, Liu H, Ma Y and Chen C 2022 *Natl. Sci. Rev.* **9** nwab168
[22] Liu H, Naumov I I, Hoffmann R, Ashcroft N and Hemley R J 2017 *Proc. Natl. Acad. Sci. USA* **114** 6990
[23] Liu S, Gao P, Hermann A, Yang G, Lü J, Ma Y, Mao H K and Wang Y 2022 *Sci. Bull.* **67** 971
[24] Zhong X, Sun Y, Iitaka T, Xu M, Liu H, Hemley R J, Chen C and Ma Y 2022 *J. Am. Chem. Soc.* **144** 13394
[25] Cui W and Li Y 2019 *Chin. Phys. B* **28** 107104
[26] Shuai H S D, Liu Y X, Wang C, Chen X, Sun H R and Liu X B 2023 *Chin. Phys. B* **32** 16101
[27] Kresse G and Furthmüller J 1996 *Phys. Rev. B* **54** 11169
[28] Perdew J P and Wang Y 1992 *Phys. Rev. B* **45** 13244
[29] Perdew J P, Burke K and Ernzerhof M 1996 *Phys. Rev. Lett.* **77** 3865
[30] Togo A, Oba F and Tanaka I 2008 *Phys. Rev. B* **78** 134106
[31] Pan S, Huang T, Vazan A, Liang Z, Liu C, Wang J, Pickard C J, Wang H T, Xing D and Sun J 2023 *Nat. Commun.* **14** 1165
[32] Nettelmann N, Helled R, Fortney J and Redmer R 2013 *Planet. Space Sci.* **77** 143
[33] French M, Mattsson T R and Redmer R 2010 *Phys. Rev. B* **82** 174108
[34] Chau R, Hamel S and Nellis W J 2011 *Nat. Commun.* **2** 203
[35] Nellis W 2017 *J. Phys.: Conf. Ser.* **950** 042046
[36] Dorn C, Hinkel N R and Venturini J 2017 *Astron. Astrophys.* **597** A38
[37] Van Hoolst T, Noack L and Rivoldini A 2019 *Adv. Phys. X* **4** 1630316